THE JOURNAL OF BIOLOGICAL CHEMISTRY VOL. 285, NO. 46, pp. 35654–35664, November 12, 2010

Tgfβ Signaling Directly Induces *Arf* Promoter Remodeling by a Mechanism Involving Smads 2/3 and p38 MAPK*[S]

Received for publication, March 31, 2010, and in revised form, August 27, 2010 Published, JBC Papers in Press, September 8, 2010, DOI 10.1074/jbc.M110.128959

Yanbin Zheng[‡], Yi D. Zhao[‡], Melissa Gibbons[‡], Tatiana Abramova[‡], Patricia Y. Chu[‡], John D. Ash[§1], John M. Cunningham[‡], and Stephen X. Skapek[‡2]

From the [‡]Department of Pediatrics, Section of Hematology/Oncology and Stem Cell Transplantation, The University of Chicago, Chicago, Illinois 60637 and the [§]Department of Ophthalmology, Dean McGee Eye Institute, University of Oklahoma Health Sciences Center, Oklahoma City, Oklahoma 73104

We have investigated how the *Arf* gene product, p19^{Arf}, is activated by Tgfβ during mouse embryo development to better understand how this important tumor suppressor is controlled. Taking advantage of new mouse models, we provide genetic evidence that *Arf* lies downstream of Tgfβ signaling in cells arising from the *Wnt1*-expressing neural crest and that the anti-proliferative effects of Tgfβ depend on *Arf in vivo*. Tgfβ1, -2, and -3 (but not BMP-2, another member of the Tgfβ superfamily) induce p19^{Arf} expression in wild type mouse embryo fibroblasts (MEFs), and they enhance *Arf* promoter activity in *Arf*$^{lacZ/lacZ}$ MEFs. Application of chemical inhibitors of Smad-dependent and -independent pathways show that SB431542, a Tgfβ type I receptor (TβrI) inhibitor, and SB203580, a p38 MAPK inhibitor, impede Tgfβ2 induction of *Arf*. Genetic studies confirm the findings; transient knockdown of Smad2, Smad3, or p38 MAPK blunt Tgfβ2 effects, as does Cre recombinase treatment of *Tgfbr2*$^{fl/fl}$ MEFs to delete Tgfβ receptor II. Chromatin immunoprecipitation reveals that Tgfβ rapidly induces Smads 2/3 binding and histone H3 acetylation at genomic DNA proximal to *Arf* exon 1β. This is followed by increased RNA polymerase II binding and progressively increased *Arf* primary and mature transcripts from 24 through 72 h, indicating that increased transcription contributes to p19^{Arf} increase. Last, *Arf* induction by oncogenic Ras depends on p38 MAPK but is independent of TβrI activation of Smad 2. These findings add to our understanding of how developmental and tumorigenic signals control *Arf* expression *in vivo* and in cultured MEFs.

Arf is conserved in amniotes as a gene encoding p19^{Arf} (p14^{ARF} in humans), a tumor suppressor that exerts its effects by both p53-dependent and -independent mechanisms (1). Early studies, predominantly in cultured cells, showed that *Arf* is induced to check proliferation in sequentially passed MEFs[3] *in vitro* (2, 3). Moreover, *Arf* expression is augmented in the presence of certain oncoproteins, like adenovirus E1A, Myc, E2F, Bcr-Abl, and Ras^{V12} (3–7). These findings coupled with the initial failure to identify *Arf* expression in the developing mouse embryo (8) led to the concept that *Arf* acts as an oncogene sensor that is induced by cell autonomous mechanisms in response to inappropriate or excessive cell proliferation signals (9).

More recent observations point toward *Arf* regulators extending beyond oncogenic signals. For instance, mouse *Arf* expression increases with age in a variety of cells that have not suffered overt oncogenic stress (10). Closer evaluation of the developing mouse embryo shows *Arf* to be robustly expressed in a temporally and spatially restricted pattern in the developing hyaloid vessels and cornea in the eye and also in perivascular cells flanking the intra-embryonic umbilical vessels (11, 12). A developmental function of p19^{Arf} is only clear in the pericyte-like cells in the hyaloid vessels of the primary vitreous, where it prevents overgrowth of the pericytes to prompt the developmentally timed regression of the hyaloid vessels (12). Homozygous *Arf* deletion results in primary vitreous hyperplasia, ocular lens opacification, retinal dysplasia, and blindness by 2 weeks of age (11, 12).

The expanded role of p19^{Arf} in the embryo raises the question of how developmental signals operate and whether they overlap with oncogenic signals controlling *Arf*. Using a candidate-gene approach, transforming growth factor β2 (Tgfβ2), a member of the Tgfβ cytokine superfamily, was recently found to be critical for *Arf* expression at several sites in the developing mouse (13). Supporting the importance of this finding, mouse embryos lacking *Tgfβ2* have primary vitreous hyperplasia similar to that observed in *Arf*$^{-/-}$ embryos (14, 15). Importantly, these observations can be replicated *in vitro* because exogenous Tgfβ2 enhances *Arf* expression in cultured MEFs and maintains a proliferation arrest in an *Arf*-dependent manner (13), thereby providing a model system to further investigate mechanisms.

Members of the Tgfβ superfamily frequently modulate the transcription of key target genes through Smad proteins, which directly transduce Tgfβ receptor activation to the nucleus. In addition, Smad-independent signaling through p38 MAPK, ERK, PI3K/Akt, and JNK provide alternative mechanisms of gene activation (16). In this manuscript we demonstrate that Tgfβ and p19^{Arf} act on cells of the same lineage; that *Arf* is required for the anti-mitogenic effects of Tgfβ *in vivo* and that

* This work was supported, in whole or in part, by National Institutes of Health Grants R01 EY0194368 and EY019942 (NEI, to S. X. S.).
[S] The on-line version of this article (available at http://www.jbc.org) contains a supplemental figure.
[1] Supported by American Diabetes Association Grant 1-06-RA-05) (to J. D. A.).
[2] To whom correspondence should be addressed: Dept. of Pediatrics, Section of Hematology/Oncology and Stem Cell Transplantation, University of Chicago, KCBD-5102, 900 E. 57th St., Chicago, IL 60637. Tel.: 773-834-3508; E-mail: sskapek@peds.bsd.uchicago.edu.
[3] The abbreviations used are: MEF, mouse embryo fibroblast; RNA Pol II, RNA polymerase II; TβrI and TβrII, Tgfβ type I and type II receptors, respectively.

both Smad- and p38 MAPK-dependent mechanisms underlie *Arf* induction by Tgfβ.

EXPERIMENTAL PROCEDURES

Animals, Cell Lines, and Reagents—$Arf^{fl/+}$ (17), $Arf^{Gfp/+}$ (18), and $Arf^{lacZ/+}$ (13) mice were maintained in a mixed C57BL/6 × 129/Sv genetic background. $Tgfβ2^{+/-}$ mice (14) were purchased from The Jackson Laboratory (Bar Harbor, ME). $Tgfbr2^{fl/fl}$ mice (19) were obtained from A. Chytil and H. L. Moses (Vanderbilt University). *AC-Tgfβ1* transgenic mice were previously described (20). *Wnt1-Cre* transgenic mice were purchased from The Jackson Laboratory (stock #003829). Primary MEFs from wild type (WT), $Arf^{lacZ/lacZ}$, and $Tgfbr2^{fl/fl}$ mice were obtained and cultivated as previously described (8). Animal studies were approved by the University of Chicago Animal Care and Use Committee.

Tgfβ1, -2, and -3 and BMP-2 were purchased from R&D Systems, Inc. (Minneapolis, MN). The siRNA targeting Smads 2 and 3, p38 MAPK, and control reagents were from Dharmacon, Inc. (Lafayette, CO). Anisomycin, SB203580, SP600125, U0126, and LY294002 (EMD Chemicals Inc; Gibbstown, NJ) and SB431542 (Tocris Bioscience; Ellisville, MO) were used in some experiments involving MEFs. β-Galactosidase in cultured cells was measured using a commercially available kit (Applied Biosystems; Foster City, CA). Adenovirus vectors encoding red fluorescent protein and Cre recombinase were produced in our laboratory using vectors provided by T. C. He (University of Chicago). Murine stem cell virus-based retrovirus vectors encoding human $H\text{-}RAS^{V12}$ were produced in our laboratory using vectors from Addgene (Cambridge, MA). Antibodies used in Western blotting experiments were directed against the following: Smad2/3, phospho-Smad2, phospho-p38 MAPK, phospho-Akt, phospho-p44/42 MAPK, and phospho-JNK (Cell Signaling Technology; Danvers, MA); TβrII and Hsc70 (Santa Cruz Biotechnology, Inc.; Santa Cruz, CA); $p19^{Arf}$ (Abcam Inc; Cambridge, MA).

Histology Studies—Female mice pregnant with embryonic day (E) 13.5 litters received BrdU (10 mg/g in PBS) by intraperitoneal injection 4 and 2 h before euthanasia using CO_2. Whole embryos were fixed in 4% paraformaldehyde in PBS for 4 h at 4 °C and then equilibrated in 20% sucrose overnight at 4 °C. Fixed embryo heads were embedded in TBS Tissue Freezing Media (Fisher) before cryostat sectioning. Hematoxylin- and eosin-staining was performed using 5-μm sections as previously described (2, 3). For BrdU staining, 5-μm sections were blocked in 10% donkey serum, 0.1% Triton X-100, PBS at room temperature and then stained using sheep α-BrdU polyclonal antibody (1:100, Fitzgerald Industries International; Action, MA) at room temperature for 90 min. The primary antibody was detected with a Dylight 488-conjugated donkey anti-sheep secondary antibody (Jackson ImmunoResearch Laboratories, Inc., West Grove, PA). Sections were mounted in VectaShield mounting media with DAPI (Vector Laboratories, Inc; Burlingame, CA) and visualized using a Leica DM IRB fluorescent microscope at 400× magnification. The fraction of DAPI-positive cells in the vitreous that were BrdU-positive was determined using at least three embryos from two or more different litters. Quantification was verified by two individuals who were blinded to the genotypes. Photomicrographs were obtained using an Optronics camera and MagnaFire 2.1C imaging software (Optronics, Goleta, CA).

Cell Culture, Western Blot Analysis, and β-Galactosidase Assay—Early passage wild type and $Arf^{lacZ/lacZ}$ MEFs were treated with either Tgfβ1 (5 ng/ml), Tgfβ2 (5 ng/ml), Tgfβ3 (10 ng/ml), or BMP2 (150 ng/ml) or an equivalent volume of vehicle (4 mM HCl) for 1.5–72 h. *Arf*-null 10T1/2 cells were transduced with *Gfp*- or *Arf*-expressing retrovirus as negative and positive controls for Western blotting. In some experiments SB203580 (20 μM), SB431542 (10 μM), SP600125 (10 μM), U0126 (10 μM), and LY 294002 (5 μM) were applied to MEFs for 20 min before Tgfβ2 or vehicle was added to the culture media. In some studies, wild type MEFs or $Arf^{lacZ/lacZ}$ MEFs were seeded at 50% confluence in 6- or 12-well plates 24 h before transfection using of siRNA targeting specific genes (or scrambled siRNA as a control) (0.5 μM) using DharmaFECT 2 (Dharmacon) according to the manufacturer's instructions. In some studies, $Tgfbr2^{fl/fl}$ MEFs were infected with adenovirus encoding Cre recombinase or red fluorescent protein as a control for 48 h before exposure to vehicle or Tgfβ2 for Western blotting for $p19^{Arf}$. In some experiments, early passage wild type MEFs were infected with retrovirus encoding $H\text{-}RAS^{V12}$ and treated with SB203580 (20 μM) and SB431542 (10 μM) concurrently. For all studies Western blotting and β-galactosidase assays were performed in wild type and $Arf^{lacZ/lacZ}$ MEFs, respectively, as previously described (13). Experimental findings were confirmed in at least two independent experiments, with quantitative data from β-galactosidase assays pooled from all representative experiments.

As a control for SB203580 activity, the p38 MAPK assay (Cell Signaling Technology) was used according to the manufacturer's instructions. Briefly, phosphorylated p38 MAPK was immunoprecipitated from the corresponding cell lysate, and its activity was determined by *in vitro* kinase assay measuring phosphorylation of its substrate ATF-2.

Chromatin Immunoprecipitation (ChIP)—For ChIP experiments, wild type MEFs (3×10^6/ChIP) were treated with Tgfβ2 (5 ng/ml) or vehicle for 1.5 h or 24 h. Cells were cross-linked and sonicated as previously described (13) and then subjected to immunoprecipitation using anti-Smad2/3 antibody (sc6033, Santa Cruz Biotechnology), anti-acetylated histone H3 (06-599, Millipore, Billerica, MA), or anti-RNA polymerase II (sc899, Santa Cruz). Goat IgG (AB-108-C, R&D Systems) and rabbit IgG (sc2027, Santa Cruz) were used as negative controls. Protein A/G-Sepharose beads (sc2003, Santa Cruz) were used to collect the protein-chromatin complexes. The beads were washed sequentially with low salt, high salt, LiCl, and TE buffers (Upstate ChIP kit, Millipore) and eluted in 0.1 M $NaHCO_3$, 1% SDS. Cross-linking was reversed by incubation at 67 °C overnight, and the genomic DNA was extracted using Qiagen PCR purification kit. A total of 7% of the precipitated DNA and 1% input DNA was amplified by PCR using primer sets for different regions of *Arf* (distal, 5′-TTCCAGGCCTTGCCATCTTCCTAT-3′ (forward) and 5′-TGGTCTGGCTGCAGTAAAGTAGCA-3′ (reverse); proximal, 5′-AGATGGGCGTGGAGCAAAGAT-3′ (forward) and 5′-ACTGTGACAAGCGAGGTGAGAA-3′ (reverse); *Nedcin* (5′-GGTCCTGCTCTGATCCG-

AAG-3′ (forward) and 5′-GGGTCGCTCAGGTCCTTACTT-3′ (reverse)). Immunoprecipitated DNA was amplified and quantified using Fast SYBR Green Master mix and the StepOnePlus real-time PCR system (both from Applied Biosystems). Results are pooled from two or three individual experiments.

Quantitative RT-PCR for Arf Expression—Total RNA extraction and cDNA preparation were accomplished using RNeasy (Qiagen) and Superscript III RT (Invitrogen) according to the manufacturer's recommendations. Quantitative RT-PCR was performed using Fast SYBR Green Master mix and the StepOnePlus real-time PCR system (both from Applied Biosystems). The following gene-specific primers were used: mature *Arf* transcript, 5′-TTCTTGGTGAAGTTCGTGCGATCC-3′ (forward) and 5′-CGTGAACGTTGCCCATCATCATCA-3′ (reverse); primary *Arf* transcript, 5′-TGGCCATAGAGGTGAACCCTTCTT-3′ (forward) and 5′-ATCCTGCACCGAGAAAGCACTGAA-3′ (reverse); *Gapdh* mature transcript, 5′-TCAACAGCAACTCCCACTCTTCCA-3′ (forward) and 5′-ACCCTGTTGCTGTAGCCGTATTCA-3′ (reverse). Results are pooled from three separate experiments.

Statistical Analysis—Quantitative data are presented as the mean ± S.D. from three or more representative experiments. Statistical significance (p value <0.05) was calculated using Student's t test.

RESULTS

Arf Is Required for Anti-proliferative Effects of Tgfβ in Vivo—*Arf* expression is blunted in the developing eyes of $Tgf\beta2^{-/-}$ embryos (13), and both $Arf^{-/-}$ and $Tgf\beta2^{-/-}$ embryos have primary vitreous hyperplasia evident at embryonic day (E) 13.5 (13, 15, 21). These observations imply that Tgfβ2 lies "upstream" of *Arf*. Furthermore, they are consistent with the idea that $p19^{Arf}$ is required for the anti-proliferative effects of Tgfβ2 in the mouse eye. To formally test this hypothesis, we took advantage of a transgenic mouse line in which Tgfβ1 is expressed from the αA-crystallin promoter (here called *AC-Tgfβ1* mice) (20). Indeed, previous studies demonstrated that transgenic expression of Tgfβ1 can rescue the *Tgfβ2*-dependent primary vitreous hyperplasia in E18.5 embryos, although the mechanism for the rescue has not been elucidated (22). This finding coupled with our prior observation that Tgfβ1 can activate the *Arf* promoter in cultured MEFs in a manner comparable with Tgfβ2 (13) allowed us to explore the epistatic relationship between *Tgfβ2* and *Arf in vivo*.

Histological examination of eyes from E13.5 embryos revealed vitreous hyperplasia restricted to the $Arf^{Gfp/Gfp}$ and $Tgf\beta2^{-/-}$ embryos as compared with their heterozygous littermates (Fig. 1, *A* and *B*). Hyperplasia was associated with increased BrdU incorporation in cells in the primary vitreous (Fig. 1, *C* and *D*). Ectopic Tgfβ1 blunted the excess proliferation in $AC\text{-}Tgf\beta1^{+}, Tgf\beta2^{-/-}$ embryos as compared with $Tgf\beta2^{-/-}$ embryos (Fig. 1*D*, *top panel*). In contrast, the $Arf^{-/-}$ defect and deregulated cell proliferation was unchanged in E13.5 $AC\text{-}Tgf\beta1^{+}, Arf^{-/-}$ embryos at E13.5 (Fig. 1, *B* and *D*, *bottom panel*). Hence, the capacity for Tgfβ1 to arrest proliferation *in vivo* depends on *Arf* and illustrates the fact that Tgfβ2 lies upstream of *Arf*.

Arf-expressing Cells in the Eye Originate from Wnt1-expressing Neural Crest—The fact that some *Arf*-expressing cells co-express TβrII in the eye (13) indicates that Tgfβ2 might signal directly to cells expressing $p19^{Arf}$. To further address this, we took advantage of the fact that members of the Sommer laboratory (23) previously showed that blocking Tgfβ signals in cells derived from a *Wnt1*-expressing lineage leads to primary vitreous hyperplasia. This was accomplished by breeding *Wnt1-Cre* mice into the $Tgf\beta r2^{fl/fl}$ mouse strain in which exon 4 *Tgfbr2* can be conditionally deleted by Cre-mediated recombination (19). We investigated whether primary vitreous hyperplasia would similarly occur in animals in which *Arf* is inactivated in the same lineage.

We accomplished this by breeding *Wnt1-Cre* mice with animals in which with exon 1β of *Arf* is flanked by LoxP sites (17). These $Arf^{fl/fl}$ animals were previously used with $Arf^{Cre/Cre}$ and $Pdgfr\beta^{fl/fl}$ animals by Gromley *et al.* (17) to formally show that conditional deletion of *Pdgfrβ* anatomically and functionally rescues the postnatal $Arf^{-/-}$ eye phenotype. As a control, we confirmed that Cre promoted recombination in cells populating the primary vitreous by analyzing *Wnt1-Cre*, $Rosa26^{lacZ/+}$ mouse embryos.[4]

Histological examination of eyes from postnatal day (P) 15 *Wnt1-Cre*, $Arf^{fl/fl}$ mice revealed a hyperplastic retrolental mass that was not observed in *Wnt1-Cre*, $Arf^{fl/+}$ or $Arf^{fl/fl}$ littermates (Fig. 2*A*; additional data not shown). Vitreous hyperplasia was also observed in *Wnt1-Cre*, $Arf^{fl/fl}$ embryos at E13.5 (Fig. 2*B*), and this correlated with increased BrdU incorporation in these cells (Fig. 2, *C* and *D*); both of these findings reflect the phenotype of $Arf^{-/-}$ mice (11, 21). This finding demonstrates that the cells that are controlled by $p19^{Arf}$ arise in the *Wnt1* expressing neural crest and further supports a model in which Tgfβ directly influences the cells expressing *Arf*.

Tgfβ1, -2, and -3 Induce $p19^{Arf}$ Expression in Cultured MEFs—Having confirmed the functional relationship between these two proteins, we sought to better define the mechanisms by which Tgfβ controls *Arf*. We took advantage of a cell culture system using early passage MEFs from wild type E14.5 embryos. To understand the kinetics of $p19^{Arf}$ induction, we treated the MEFs with Tgfβ2 for 1.5, 24, and 48 h. In this context, $p19^{Arf}$ protein was minimally increased at 24 h and was significantly higher at 48 h (Fig. 3*A*), suggesting that $p19^{Arf}$ induction was not an immediate Tgfβ2 response.

We also measured the ability of each of the closely related Tgfβ1, -2, and -3 proteins to enhance *Arf* expression by using MEFs derived from an $Arf^{lacZ/lacZ}$ reporter mouse in which the first exon of *Arf* is replaced by *lacZ* cDNA (13). $Arf^{lacZ/lacZ}$ MEFs derived are functionally $Arf^{-/-}$, and β-galactosidase expression can be used as a surrogate for *Arf* promoter activity. Our previous work showed that the time course for β-galactosidase induction by Tgfβ2 parallels that of $p19^{Arf}$ protein (Fig. 3*A*) (13). All three of the related Tgfβ proteins induced β-galactosidase expression in the MEFs (Fig. 3*B*, *lanes 2*, *4*, and *6*). The relatively small increases in the *Arf* promoter in $Arf^{lacZ/lacZ}$ MEFs as compared with $p19^{Arf}$ induction (compare Fig. 3, *A*,

[4] S. X. Skapek, unpublished data.

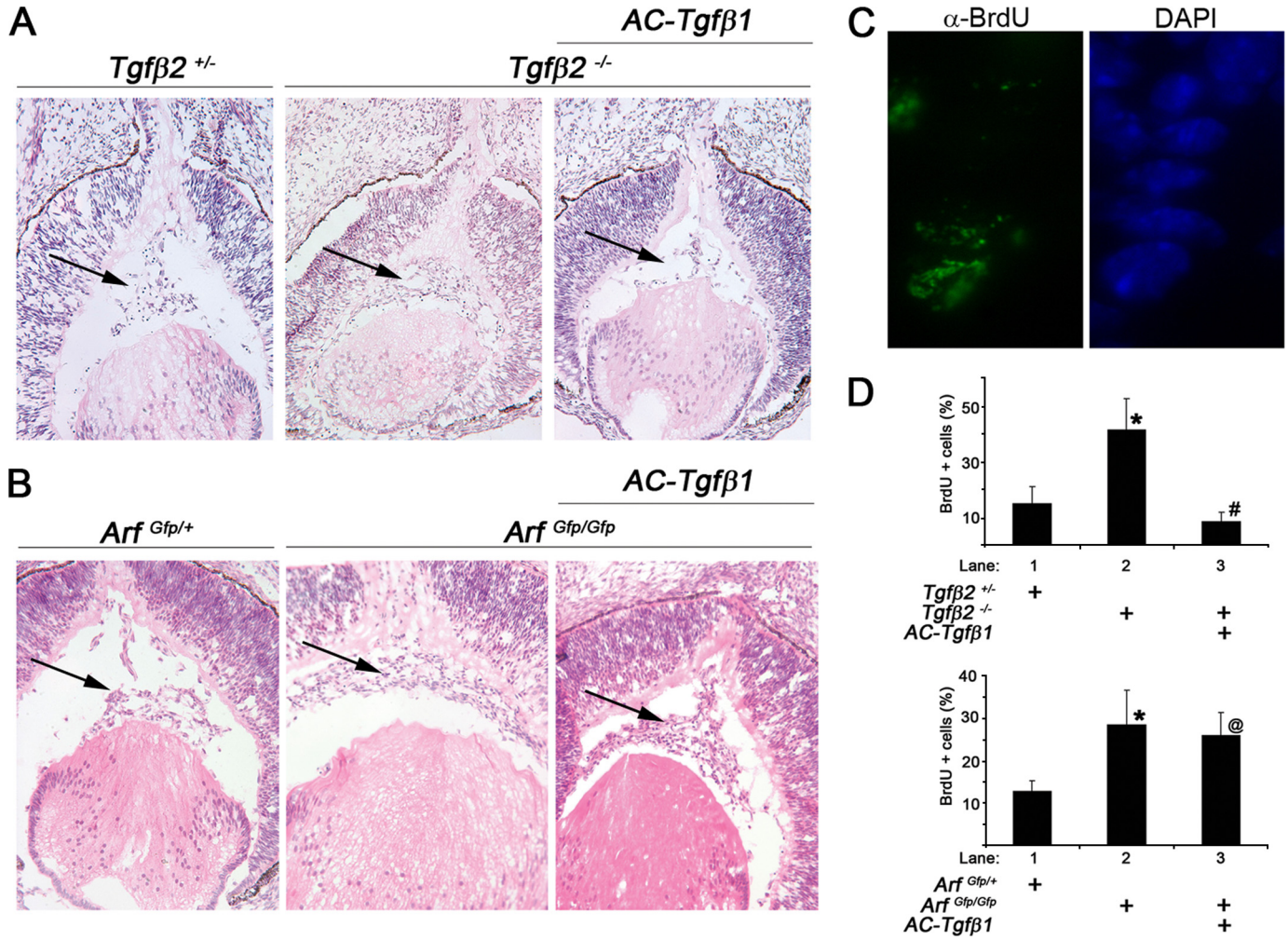

FIGURE 1. **Arf is required for the anti-proliferative effects of Tgfβ1 during eye development.** *A* and *B*, representative photomicrographs of hematoxylin- and eosin-stained slides of E13.5 embryos showing the primary vitreous hyperplasia in *Tgfβ2*$^{-/-}$ and *Arf*$^{-/-}$ embryos (*middle panels*) is corrected by ectopic Tgfβ1 in *AC-Tgfβ1* animals only when *Arf* is present (*right panels*). *Arrows* denote the cellular area of the primary vitreous. *C* and *D*, shown are a representative photomicrograph (*C*) and quantification (*D*) of BrdU incorporation in the vitreous of E13.5 mouse embryo eyes of the indicated genotypes. Original magnification: 200× (*A* and *B*); 400× (*C*). Quantitative data are expressed as average percent of total cells in the vitreous space. Increased proliferation in absence of *Arf* or *Tgfβ2* is statistically significant (*lane 2 versus 1*; *). $p < 0.002$ (*top*) and <0.01 (*bottom*). Decreased proliferation by ectopic expression of Tgfβ1 was not significant in the absence of *Arf* (*lane 3 versus* 2). $p < 0.001$ (*top*, #) and $p = 0.35$ (*bottom*, @).

lanes 5 and *6* to *B*, *lanes 3* and *4*) indicated that increased *Arf* transcription might be complemented by additional, post-transcription effects such as transcript stabilization or increased translation. In contrast, BMP-2, another Tgfβ superfamily member (16, 24), failed to induce β-galactosidase (Fig. 3*C*). These findings suggest that Tgfβ1, -2, or -3 act through the classical pathway involving ALK-5 and TβrII rather than BMP type I receptors (ALK-2, ALK-3, and ALK-6) (16, 24).

We previously showed *Arf* and TβrII to be co-expressed in some pericyte-like cells in the primary vitreous in the mouse (13). To directly confirm the importance of this receptor in *Arf* gene activation, we used MEFs derived from the above-mentioned *Tgfbr2*$^{fl/fl}$ mouse. When the MEFs were infected with adenovirus encoding Cre recombinase, TβrII expression fell (Fig. 3*D*, *lanes 3* and *4 versus 1* and *2*). Tgfβ2 augmented p19^{Arf} in *Tgfbr2*$^{fl/fl}$ MEFs when they were infected with control adenovirus encoding red fluorescent protein (Fig. 3*D*, *lane 2 versus lane 1*) but not in MEFs in which Cre recombinase had diminished TβrII expression (Fig. 3*D*, *lane 4 versus lane 3*).

Smads 2 and 3 Cooperatively Induce p19^{Arf} *in Response to Tgfβ2*—Given the role that Smads 2 and 3 play in response to Tgfβ2, we sought to define the relative importance of these two proteins in *Arf* regulation. We used gene-specific siRNA to knock down their expression singly and in combination in wild type and *Arf*$^{lacZ/lacZ}$ MEFs (Fig. 4, *A* and *B*, *top panel*; the supplemental figure). Despite the very low Smad3 expression as compared with Smad 2, knockdown of either one impaired Tgfβ2 induction of the native *Arf* locus and β-galactosidase in wild type and *Arf*$^{lacZ/lacZ}$ MEFs, respectively; interestingly, targeting both proteins further limited *Arf* induction (Fig. 4, *A* and *B*, *bottom panel*). These findings indicate that Smad2 and -3 cooperatively control *Arf* induction by Tgfβ2.

The p38 MAPK-dependent Pathway Also Mediates Tgfβ2 Effects on p19^{Arf}—To investigate whether Smad-independent signals also influence Tgfβ2 induction of p19^{Arf}, we used a panel of chemical inhibitors targeting a variety of pathways recognized to be influenced by Tgfβ (Fig. 5*A*). As a control, we included SB431542, an inhibitor of TβrI, which blocks Smad2

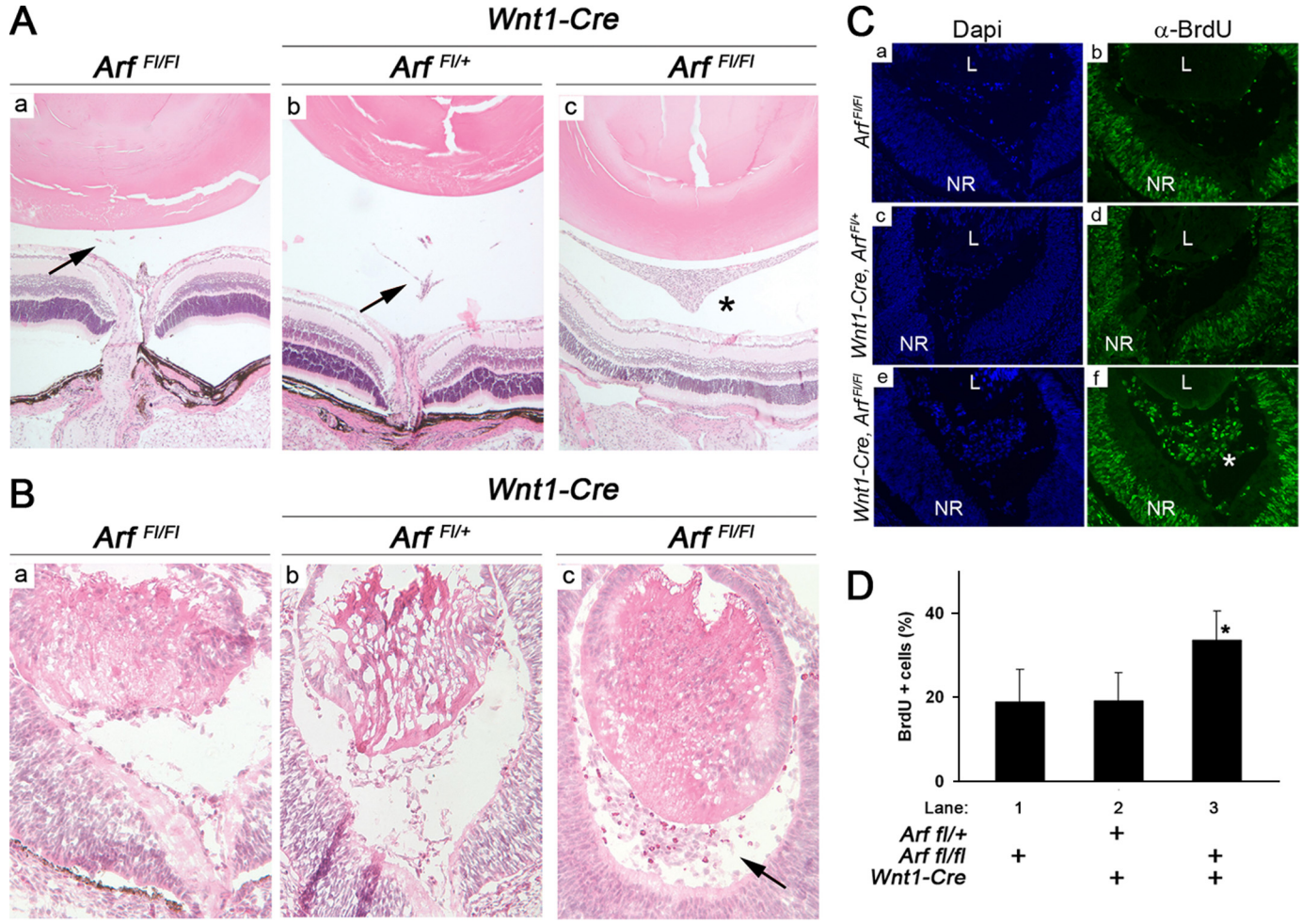

FIGURE 2. **Conditional loss of *Arf* in *Wnt1*-expressing neural crest cells causes primary vitreous hyperplasia.** *A* and *B*, shown are representative photomicrographs of hematoxylin- and eosin-stained sections through $Arf^{fl/fl}$ (*a*), *Wnt1-Cre*, $Arf^{fl/+}$ (*b*), and *Wnt1-Cre*, $Arf^{fl/fl}$ (*c*) eyes at P15 (*A*) and at E13.5 (*B*). Hyperplastic retrolental mass observed in the postnatal period (*A*, *) is evident as early as E13.5 (*B*, *arrow*). *Arrows* (*A*) indicate remnants of normal, regressing hyaloid vessels when functional $p19^{Arf}$ is present. *C* and *D*, shown are representative photomicrographs (*C*) and quantification (*D*) of BrdU incorporation in the vitreous E13.5 mouse embryo eyes of the indicated genotypes. Note the expansion of BrdU-positive, proliferating cells (*C*, *) in the primary vitreous between the lens (*L*) and the neuroretina (*NR*) in *Wnt1-Cre*, $Arf^{fl/fl}$ mice. Quantitative data are expressed as average percent of total cells in the vitreous space. Increased BrdU+ cells in *Wnt1-Cre*, $Arf^{fl/fl}$ embryos (*D*, *lane 3*) is statistically significant. $p < 0.001$(*) for *lane 3 versus lanes 1* or *2*).

phosphorylation and Tgfβ2-driven induction of $p19^{Arf}$ and *lacZ* expression in wild type and $Arf^{lacZ/lacZ}$ MEFs, respectively (13) (Fig. 5, *B*, *lanes 5* and *6*, C, *lanes 11* and *12*, and *D*, *lane 7*).

Application of SB203580, a chemical inhibitor of p38 MAPK, blunted *Arf* expression in both models (Fig. 5, *B*, *lanes 3* and *4*, and *C*, *lanes 3* and *4*) but did not interfere with Smad 2 phosphorylation (Fig. 5*D*, *lane 3*). Consistent with a previous publication, SB203580 was not able to block p38 MAPK phosphorylation (25, 26), but it did block the phosphorylation of its downstream target ATF-2 (Fig. 5*E*). Of note, blocking TβrI activity with SB431542 also dampened p38 MAPK activation, consistent with existence of parallel pathways downstream from this receptor (Fig. 5*D*, *lane 7*). Although the absence of a measurable effect on Smad2 phosphorylation suggests that SB203580 may act independently of Smads, we cannot formally exclude the possibility that p38 MAPK inhibition does influence Smad-dependent activity.

Other chemical inhibitors had less robust effects on *Arf* induction. Although p42/p44 MAPK blockade by U0126 (Fig. 5*D*, *lane 6*) modestly augmented Tgfβ2 induction of β-galactosidase in $Arf^{lacZ/lacZ}$ MEFs (Fig. 5*C*, *lane 10*), a similar effect on $p19^{Arf}$ protein was not evident in wild type MEFs (Fig. 5*B*, *lane 10*). Inhibition of PI3K/Akt by LY294002 or JNK by SP600125 had no measurable effect on *Arf* induction by Tgfβ2 (Fig. 5, *B*, *lanes 12* and *8*, and *C*, *lanes 6* and *8*) even though the compounds were active in MEFs (Fig. 5, *D*, *lane 4*, and *F*, *lane 4*).

Because SB203580 might have off-target effects, we used a genetic approach to confirm the importance of p38 MAPK in Tgfβ-mediated *Arf* regulation. Consistent with our results from chemical inhibition, even partial knockdown of p38 MAPK blocked the effects of Tgfβ2 on *Arf* expression (Fig. 6, *A* and *B*).

Tgfβ Fosters Chromatin Remodeling of the Arf Gene—We previously demonstrated Smad 2/3 had the capacity to bind to two regions ~2.2 and ~1.5 kb upstream of the *Arf* translation initiation codon in $Arf^{lacZ/lacZ}$ MEFs (13); however, we did not understand how Tgfβ2 influenced the binding, the kinetics of the effect, and any other coincident changes to the *Arf* gene. To begin to address these issues, we first examined the binding of Smad2/3 to these regions in vehicle- and cytokine-treated MEFs. We used wild type MEFs to preclude

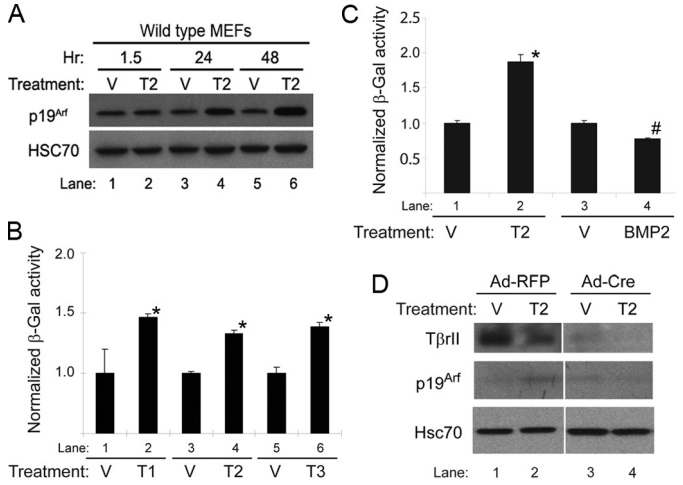

FIGURE 3. **Tgfβ1, -2, and -3 induce p19^{Arf} and the *Arf* promoter in cultured MEFs in a manner that depends on TβrII.** *A–C*, shown is a representative Western blot of lysates from wild type MEFs (*A*) and β-galactosidase (*β-Gal*) activity in *Arf*$^{lacZ/lacZ}$ MEFs (*B* and *C*) showing the time course of *Arf* induction after 48 h of exposure to Tgfβ1, -2, or -3 (*T1*, *T2*, *T3*), BMP2, or vehicle (*V*). Induction by each Tgfβ protein was statistically significant when compared with respective vehicle (*B* and *C*, *), as was the slight repression by BMP2 (*C*, #) ($p \leq 0.0002$ in each case). *D*, shown is a representative Western blot for the indicated proteins using lysates from *Tgfbr2*$^{fl/fl}$ MEFs infected with either adenovirus encoding red fluorescent protein (*RFP*) or Cre recombinase and exposed to Tgfβ2 or vehicle for 48 h. Note that p19^{Arf} induction (*lane 2 versus lane 1*) is blunted after inactivation *Tgfbr2* (*lane 4 versus lane 3*).

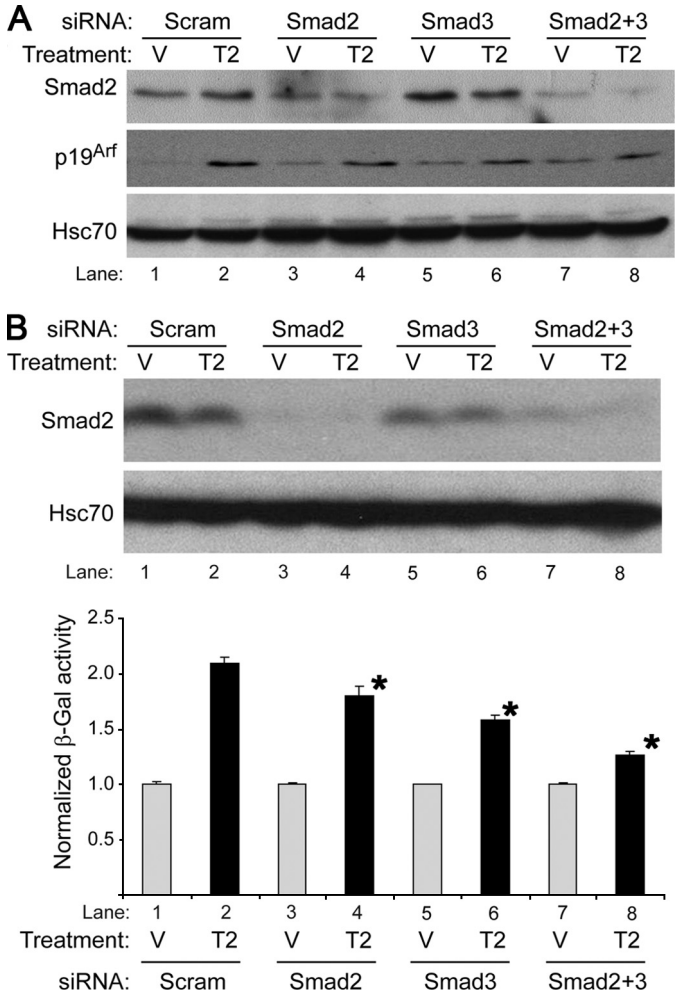

FIGURE 4. **siRNA targeting Smad2 and -3 impairs Tgfβ2 induction of *Arf*.** Shown are representative Western blots (*A* and *B*, *upper panel*) of lysates from wild type MEFs (*A*) or *Arf*$^{lacZ/lacZ}$ MEFs (*B*) and β-galactosidase assay (*β-gal*, *B*, *lower panel*) in *Arf*$^{lacZ/lacZ}$ MEFs treated with Tgfβ2 (*T2*) or vehicle (*V*) for 72 (*A*) or 60 (*B*) h after transfection with either siRNA control (*Scram*) or siRNA targeting Smad2 and/or Smad3 as indicated. Western blotting confirms partial knockdown of Smad2. (longer exposure confirming Smad3 knock-down is available as the supplemental figure). β-Galactosidase activity, normalized to expression in respective vehicle, is expressed as the average of three or more replicates from separate experiments. Knockdown of Smad2 or -3 or both significantly decreased β-galactosidase as compared with siRNA control. $p <$ 0.007 for each case (*lower panel*, *).

adverse positional effects from insertion of the *lacZ-Neo* cassette into the *Arf* locus in *Arf*$^{lacZ/lacZ}$ MEFs; however, more limited analysis of these MEFs showed essentially the same results (data not shown).

We observed that Smad2/3 binding at both the distal and proximal Tgfβ2 binding elements (formerly P3 and P7, respectively, in Freeman-Anderson *et al.* (13)) increased within 1.5 h after the addition of Tgfβ2 (Fig. 7*Ba*); the effects were more pronounced at the promoter proximal element. In contrast, Tgfβ2 did not significantly enhance Smad2/3 binding over base line at the other, previously identified distal site (formerly called P1 in Freeman-Anderson *et al.* (13)) (data not shown) or at putative Tgfβ2 binding elements in the first intron (formerly P11 in Freeman-Anderson *et al.* (13)) (Fig. 7, *A* and *Ba*, *lanes 3–6*).

Smad binding can foster histone modification and the recruitment of the RNA Polymerase II (RNA Pol II) complex at Tgfβ-responsive genes (27, 28). In our experiments, histone H3 acetylation paralleled changes in Smad2/3 binding at the distal and proximal elements 1.5 h after Tgfβ2 treatment; histone acetylation was not observed at the *Necdin* promoter, a locus that remains silent in MEFs (Fig. 7*Bb*, *lanes 1–4 versus 5* and *6*). In contrast to early Smad2/3 binding and histone acetylation, RNA Pol II binding at the proximal site was absent at 1.5 h but became detectable by 24 h after Tgfβ (Fig. 7*Bc*).

Tgfβ Treatment Increases Arf Transcription—We used quantitative, real-time RT-PCR to explore how the events at the *Arf* promoter correlated with increased transcription. The mature *Arf* mRNA transcript increased in wild type MEFs from nearly base line at 24 h through 72 h after Tgfβ2 addition to the culture media (Fig. 8, *top panel*) in a time course paralleling p19^{Arf} induction (Fig. 3*A*). Similarly, quantitative, real-time RT-PCR of the primary, unprocessed *Arf* transcript increased (Fig. 8, *bottom panel*). The parallels between RNA Pol II localization and *Arf* primary transcript induction indicate that Tgfβ2 enhances *Arf* transcription between 24 and 72 h even though Smad2/3 binding and histone modification near exon 1β are enhanced as early as 1.5 h after exposure to this cytokine.

Oncogenic RAS Activates Arf Independently of Tgfβ Signaling to Smad2/3—*Arf* was initially described as an oncogene sensor that checks inappropriate or excessive cell proliferation signals. For example, ectopic expression of oncogenic H-RAS^{V12} activates *Arf* via the Raf-ERK-Dmp1 pathway (29). We investigated whether the developmental signaling pathway outlined above was relevant to *Arf* induction by oncogenic RAS expression in MEFs.

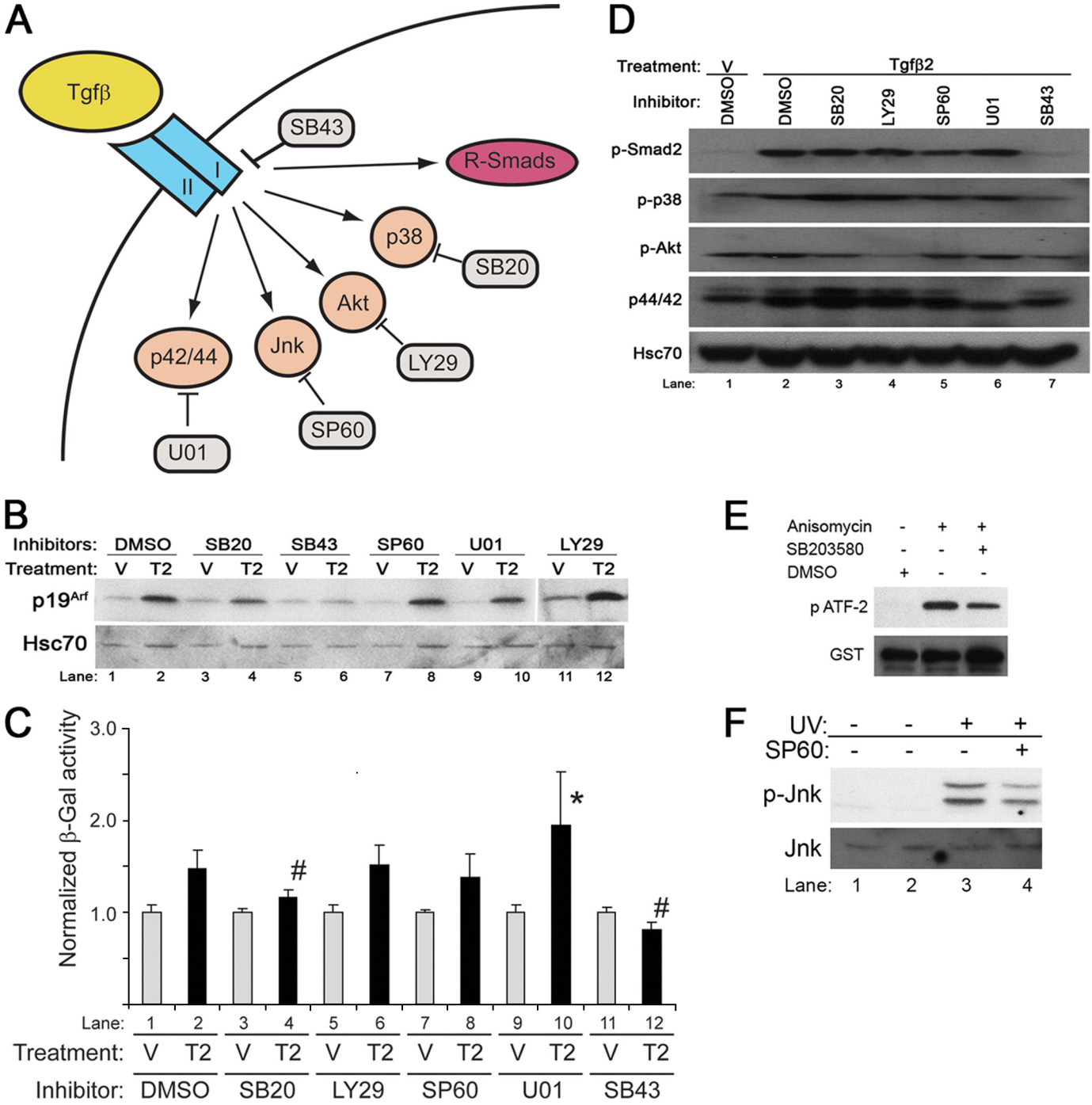

FIGURE 5. **Smad-independent pathways influence Tgfβ induction of *Arf*.** *A*, shown is a schematic diagram showing Smad-dependent and Smad-independent and specific inhibitors for each target: *SB43*, SB431542; *SB20*, SB203580; *SP60*, SP600125; *U01*, U0126; *LY29*, LY294002. *B* and *C*, shown is a representative Western blot for the indicated proteins from wild type MEFs (*B*) and β-galactosidase activity in $Arf^{lacZ/lacZ}$ MEFs (*C*) exposed to Tgfβ2 (*T2*) or vehicle (*V*) for 48 h and either DMSO or the indicated chemical inhibitors. Quantitative analysis (*C*) shows that Tgfβ2 significantly changed β-galactosidase activity when compared with relevant vehicle ($p < 0.013$); however, the induction of β-galactosidase was significantly blunted by SB203580 and SB431542 when compared with DMSO ($p = 0.0015$ (#) and <0.001 (*), respectively), and it was significantly enhanced by U0126 when compared with DMSO ($p = 0.047$ (#)). *D*, a representative Western blot shows the corresponding targets for individual inhibitors in $Arf^{lacZ/lacZ}$ MEFs exposed to Tgfβ2, and the indicated chemical inhibitor confirms that LY294002 blocks AKT phosphorylation (*lane 4*), U0126 blocks p42/44 phosphorylation (*lane 6*), and SB431542 blocks Smad2 and p38 MAPK phosphorylation (*lane 7*). *E*, representative Western blot using $Arf^{lacZ/lacZ}$ MEFs exposed to the indicated chemical inhibitors or DMSO for 20 min shows that SB20 blunts anisomycin-stimulated, p38 MAPK-dependent phosphorylation ATF-2. *F*, a representative Western blot using $Arf^{lacZ/lacZ}$ MEFs exposed SP600125 for 20 min blunts UV-stimulated phosphorylation of JNK.

Ectopic expression of human H-RAS^{V12} induced p19^{Arf} 48 h later in early passage, wild type MEFs (Fig. 9, *lanes 4 versus 1*). Inhibition of TβrI phosphorylation of Smad2/3 by SB431542 had no obvious effect *Arf* induction (Fig. 9, *lane 5 versus 2*), but it did slightly increase base-line p19^{Arf} (Fig. 9, *lane 2 versus 1*). In contrast, inhibition of p38 MAPK using SB203580 significantly blocked p19^{Arf} induction by H-RAS^{V12} (Fig. 9, *lane 6 versus 3*). Of note, p19^{Arf} induction by ectopically expressed

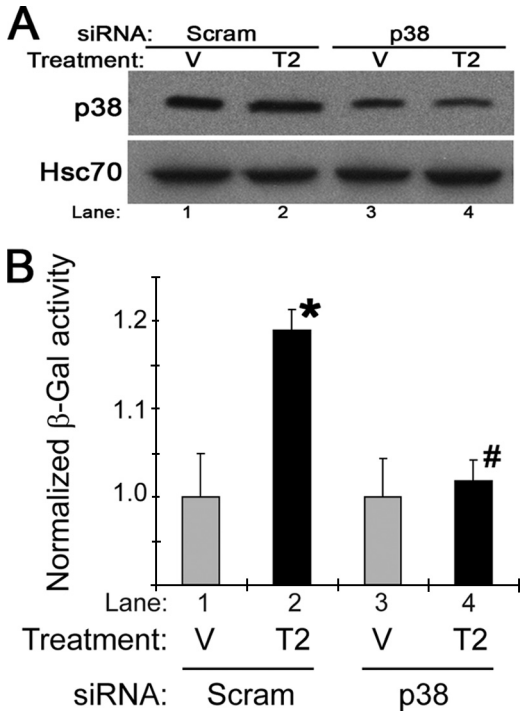

FIGURE 6. **Knockdown of p38 limits Tgfβ induction of the *Arf* promoter.** Shown is a representative Western blot (*A*) and β-galactosidase assay (*B*) of $Arf^{lacZ/lacZ}$ MEFs transfected with either siRNA control (*Scram*) or siRNA targeting p38 for 24 h before exposure to vehicle (*V*) or Tgfβ2 (*T2*) for 60 h. β-Galactosidase (*β-Gal*) induction by Tgfβ2, normalized to vehicle, was significant when compared with vehicle in control cells ($p < 0.001$ (*)) but not in cells transfected with p38 siRNA ($p = 0.31$ (#)).

cyclin D1 was not measurably affected by either chemical inhibitor.[5] Thus, p38 MAPK is needed for full induction of *Arf* by both Tgfβ2 and oncogenic RAS in MEFs; in contrast, Smad2/3 phosphorylation is only required for *Arf* induction by Tgfβ2.

DISCUSSION

The central role that $p19^{Arf}$ plays as a tumor suppressor in incipient cancer cells is well established. In contrast, relatively little is known about *Arf* regulation in physiological contexts. We recently demonstrated that the *Tgfβ2* gene is essential for *Arf* induction at several sites in the developing mouse embryo (13). Here we further explore the functional relationships between Tgfβ and $p19^{Arf}$ *in vivo*, and we uncover molecular mechanisms underlying *Arf* induction by this signaling protein.

First, we demonstrate that the capacity for Tgfβ to arrest cell proliferation *in vivo* in the developing eye strictly depends on its ability to induce $p19^{Arf}$. Hence, understanding of how it induces *Arf* becomes central to knowing how it acts in this developmental capacity. Second, we use a genetic approach to show that TβrII and $p19^{Arf}$ both act in cells of the same, neural crest-derived lineage to prevent primary vitreous hyperplasia; this provides *in vivo* evidence for cell-intrinsic signaling from TβrII to *Arf*. Third, the complementary use of chemical inhibitors and genetic manipulations define the signaling pathways extending from Tgfβ1, -2, or -3 binding to the TβrI/II complex to *Arf* gene activation. Our findings indicate that Smads 2 and 3 and p38 MAPK are necessary for full $p19^{Arf}$ induction. We have characterized the kinetics of Smad2/3 binding in DNA elements 5′ to *Arf* and subsequent changes in the chromatin architecture of the locus. Interestingly, although these events begin within a short 1.5-h timeframe after Tgfβ2 treatment, *Arf* transcription, measured by RNA Pol II binding and primary *Arf* transcript increase, are not detected until 24–48 h later. Last, we show that *Arf* induction by oncogenic RAS shares the p38 MAPK arm of this developmental pathway, whereas activation of Smad2/3 is dispensable.

The delay between Smad binding to the *Arf* gene and subsequent increases in *Arf* promoter and transcript levels was unexpected. Early Smad-dependent effects of Tgfβ on gene transcription are often evident within several hours of receptor activation (*e.g.* Gomis *et al.* 30)). Indeed, in cultured MEFs, early cell proliferation arrest by Tgfβ2 proceeds independently of *Arf* (13) and is likely mediated by earlier events like repression of Cdk4 (31) or induction of Cdk inhibitors like $p21^{Cip1}$ or $p15^{Ink4b}$ (32, 33). We can speculate that the delayed *Arf* induction (although still initiated as an immediate Smad-dependent response) could have evolved to allow $p19^{Arf}$ to primarily contribute to the maintenance of a Tgfβ-driven proliferation arrest.

At a molecular level, the delay between Smad binding and transcriptional activation suggests the need for the recruitment of other transcription factors to *Arf* regulatory sequences before or coincident with RNA Pol II binding. Candidate transcription factors already implicated as direct *Arf* regulators (by virtue of binding to the *Arf* promoter) include E2f 1 and 3 (34), Dmp1 (35), Pokemon (36), and FoxO3a (37), which positively or negatively regulate mouse *Arf* expression. Of these, FoxO3a (which binds to intronic DNA ~8 kb 3′ of exon 1β) (37) is particularly interesting because FoxO proteins directly interact with Smads 2/3 and 4 to induce $p21^{Cip1}$ (38). Functional cooperation between FoxO and Smad proteins is also found in a cluster of genes that seem to control stress and adaptive cell signaling responses at least in cultured HaCaT cells (30). However, this work focused on immediate responses within 3 h, a time point at which *Arf* transcription is not observed. In our preliminary studies, Tgfβ2 did not alter the levels of FoxO3a in MEFs, nor did inhibition of Akt (a negative regulator of FoxO (39)). Additional work is required to confirm or dispel the importance FoxO proteins in *Arf* regulation in the eye.

That a p38-dependent signaling pathway also contributes to the regulation of *Arf* by Tgfβ is consistent with the growing understanding of cross-talk between Smad-dependent and -independent effectors of Tgfβ (16). p38 MAPK has previously been implicated in *Ink4/Arf* regulation; for example, decreased expression of Wip1 phosphatase in $Ppm1d^{-/-}$ MEFs increases both $p16^{Ink4a}$ and $p19^{Arf}$ in a p38 MAPK-dependent manner (40). It also contributes to other Tgfβ effects like the arrested DNA synthesis in primary mouse vascular smooth muscle cells at 48 h (26), induction of type I collagen in a cultured retinal pigment epithelial cell line at 24 h (41), and increased α-smooth muscle actin expression at 48–72 h in cultured primary human fibroblasts (42). We previously showed that some of the *Arf*-expressing perivascular cells also express α-smooth muscle actin in the newborn mouse eye and that ectopic $p19^{Arf}$ expression in 10T1/2 fibroblasts (in which *Arf* is deleted) can promote

[5] Y. Zheng and S. X. Skapek, negative data not shown.

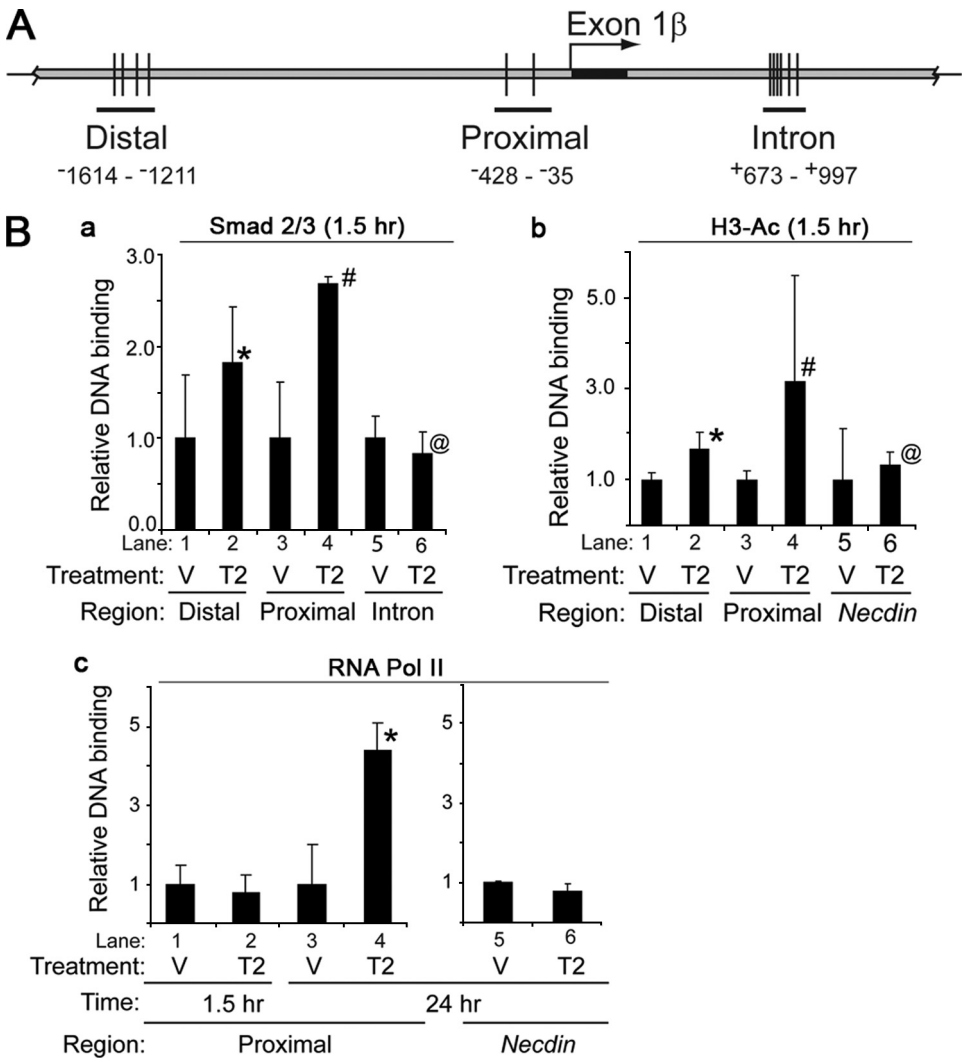

FIGURE 7. **Tgfβ2 promotes Smad2/3 binding, histone H3 acetylation, and RNA Pol II localization to the *Arf* locus in MEFs.** *A*, a schematic diagram shows Distal, Proximal. and Intron regions of *Arf* locus used in ChIP assays. *B*, shown is quantitative analysis of representative ChIP assays of using wild type MEFs exposed to vehicle (*V*) or Tgfβ2 (*T2*) for 1.5 h (*a–c*) or 24 h (*c*) after serum deprivation. A ChIP assay was carried out using antibodies specific to Smad2/3 (*a*), histone H3 acetylated at lysines 9 and 14 (*H3-Ac*) (*b*), and RNA polymerase II (*RNA Pol II*) (*c*). Immunoprecipitated DNA and input DNA were amplified with primers for genomic regions indicated in *A* or for the Tgfβ2 non-responsive gene *Necdin*. *p* values are as follows: *a*, 0.081 (*), 0.001 (#), 0.55 (@); *b*, 0.045 (*), 0.183 (#), 0.738 (@); (*c*) 0.059 (*) for Tgfβ2 *versus* corresponding vehicle.

α-smooth muscle actin and smooth muscle myosin expression 48–96 h later (43). Conceivably, the induction of *Arf* with smooth muscle proteins may represent part of a Tgfβ- and p38 MAPK-dependent transcriptional routine leading to the maturation and cell cycle arrest of a subtype of vascular smooth muscle cells surrounding the hyaloid vessels.

How Smad and p38 MAPK signaling cooperates to induce *Arf* is not clear. Direct cooperation between the two is possible, and our preliminary studies indicate that SB203580 slightly decreases Smad2/3 occupancy at the proximal element, but the decrease is not statistically significant (negative data not shown). Instead, the positive interactions we found may lie in the ability of p38 MAPK to activate potential transcriptional co-factors, such as p300, C/EBPβ, or ATF2 (16, 44, 45). Of these, p300 is known to cooperate with Smads to modulate histone acetylation (46). Putative binding sites for C/EBPβ and ATF-2 are present in genomic DNA flanking the *Arf* first exon. C/EBPβ was shown to be required for Ras^{V12}-mediated senescence in MEFs but it was not needed for $p19^{Arf}$ induction by this oncogene (47); instead, $p19^{Arf}$ negatively regulates C/EBPβ (48). ATF2 has a variety of activities that could play a role in cancer biology, but there is no clear connection to *Arf* (49).

Given the broad role of *Arf* in both tumor suppression and eye development, our findings may help us understand certain human diseases. For instance, so far the molecular pathogenesis of persistent hyperplastic primary vitreous, which the $Arf^{-/-}$ model mimics (11, 12), is unclear. Occasional familial cases of this disease suggest an underlying genetic basis (50–52). Elucidating the complete series of components necessary for Tgfβ-mediated *Arf* transcription will allow us to potentially interrogate the genomic DNA extracted from either involved tissue samples or from blood of diseased patients in a more focused way. Because a persistent hyperplastic primary vitreous-like disease can also develop in somatic mosaic mice in which *Arf* is missing in only a subset of cells in the mouse (43), such an analysis should be accomplished in a way that can also detect mosaicism of the key gene(s).

We hope that our findings may also provide some insight into tumor suppression by *Arf* in incipient, oncogene-stressed cancer cells. This may involve both how *Arf* is induced and how Tgfβ acts as a tumor suppressor. *Arf* induction by oncogenic RAS, E1A, or Myc in cultured cells occurs over ~48 h (4, 5), a time course that is similar to induction by Tgfβ (Fig. 3*A*). It is interesting that Tgfβs were initially described in oncogene-transformed fibroblasts (53, 54). Furthermore, using cultured mouse keratinocytes, $v\text{-}Ras^{Ha}$ and Tgfβ1 cooperatively induce $p19^{Arf}$ and $p16^{Ink4a}$, which is also encoded at the *Arf/Ink4a* locus, and base-line $p19^{Arf}$ expression is decreased in $Smad3^{-/-}$ keratinocytes transduced by $v\text{-}Ras^{Ha}$-transduced cells (55). These findings imply that *Arf* induction by certain oncogenes might be driven by an autocrine or paracrine loop. In our analysis of cultured MEFs, RAS^{V12} does not require TβrI/Smad signaling, although full *Arf* induction by ectopic RAS depends on p38 MAPK. Because tissue-specific factors control *Arf* induction by oncogenic Ras (56), a more robust investigation into the relationship between *Arf* regulation by Tgfβ and by different oncogenes will require analysis of a variety of cell types and contexts.

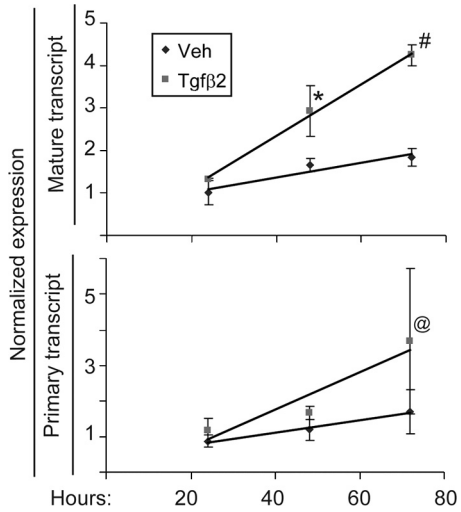

FIGURE 8. **Tgfβ2 increases both the primary and mature *Arf* transcript.** Shown is quantitative analysis of real time, RT-PCR using total RNA isolated from wild type MEFs exposed to vehicle (*Veh*) or Tgfβ2 for the indicated times. Differences in transcript level between Tgfβ2- and vehicle-treated MEFs are significant for the mature transcript at 48 and 72 h ($p < 0.04$ (*) and < 0.005 (#)) and for the primary transcript at 72 h ($p = 0.039$ (@)).

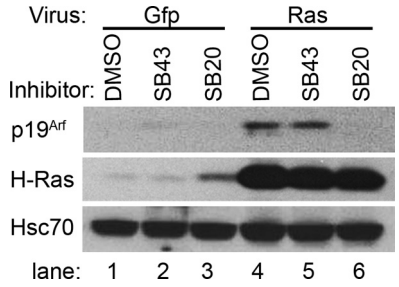

FIGURE 9. **p38 MAPK signaling is needed for *Arf* induction by ectopically expressed RAS, but inhibition of Tβrl does not.** Representative Western blot for the indicated proteins using lysates from wild type MEFs, exposed to the indicated chemical inhibitors at the time of transduction using Gfp- or H-RAS^{V12}-expressing retrovirus. Lysates were collected 48 h after transduction. Fluorescence microscopy detection of Gfp from the murine stem cell virus-based vectors showed no differences in transduction efficiency across the samples.

The anti-tumor effects of Tgfβ have been well described (57, 58), and disruption of components of the pathway is particularly common in certain cancers, like those involving the cervix, gastrointestinal epithelium, and liver (59–61). In other contexts, Tgfβ appears to promote tumorigenesis (58, 62). One might reconcile these apparent discrepancies if the presence or absence of *Arf*, which is required for anti-proliferative effects of Tgfβ2 in the eye, also determines the effectiveness of Tgfβ-mediated tumor suppression.

Acknowledgments—We gratefully acknowledge T. C. He (University of Chicago) for providing adenovirus vectors, C. J. Sherr (St. Jude Children's Research Hospital) for providing Arf$^{fl/fl}$ mice before their publication, and helpful discussions with D. Dighe, S. Volchenboum, R. Widau, and A. Zelivianskaia (all at the University of Chicago).

REFERENCES

1. Sherr, C. J. (2006) *Nat. Rev. Cancer* **6,** 663–673
2. Kamijo, T., Zindy, F., Roussel, M. F., Quelle, D. E., Downing, J. R., Ashmun, R. A., Grosveld, G., and Sherr, C. J. (1997) *Cell* **91,** 649–659
3. Zindy, F., Eischen, C. M., Randle, D. H., Kamijo, T., Cleveland, J. L., Sherr, C. J., and Roussel, M. F. (1998) *Genes Dev.* **12,** 2424–2433
4. de Stanchina, E., McCurrach, M. E., Zindy, F., Shieh, S. Y., Ferbeyre, G., Samuelson, A. V., Prives, C., Roussel, M. F., Sherr, C. J., and Lowe, S. W. (1998) *Genes Dev.* **12,** 2434–2442
5. Lin, A. W., and Lowe, S. W. (2001) *Proc. Natl. Acad. Sci. U.S.A.* **98,** 5025–5030
6. Palmero, I., Pantoja, C., and Serrano, M. (1998) *Nature* **395,** 125–126
7. Williams, R. T., Roussel, M. F., and Sherr, C. J. (2006) *Proc. Natl. Acad. Sci. U.S.A.* **103,** 6688–6693
8. Zindy, F., Quelle, D. E., Roussel, M. F., and Sherr, C. J. (1997) *Oncogene* **15,** 203–211
9. Lowe, S. W., and Sherr, C. J. (2003) *Curr. Opin. Genet. Dev.* **13,** 77–83
10. Krishnamurthy, J., Torrice, C., Ramsey, M. R., Kovalev, G. I., Al-Regaiey, K., Su, L., and Sharpless, N. E. (2004) *J. Clin. Invest.* **114,** 1299–1307
11. McKeller, R. N., Fowler, J. L., Cunningham, J. J., Warner, N., Smeyne, R. J., Zindy, F., and Skapek, S. X. (2002) *Proc. Natl. Acad. Sci. U.S.A.* **99,** 3848–3853
12. Martin, A. C., Thornton, J. D., Liu, J., Wang, X., Zuo, J., Jablonski, M. M., Chaum, E., Zindy, F., and Skapek, S. X. (2004) *Invest. Ophthalmol. Vis. Sci.* **45,** 3387–3396
13. Freeman-Anderson, N. E., Zheng, Y., McCalla-Martin, A. C., Treanor, L. M., Zhao, Y. D., Garfin, P. M., He, T. C., Mary, M. N., Thornton, J. D., Anderson, C., Gibbons, M., Saab, R., Baumer, S. H., Cunningham, J. M., and Skapek, S. X. (2009) *Development* **136,** 2081–2089
14. Sanford, L. P., Ormsby, I., Gittenberger-de Groot, A. C., Sariola, H., Friedman, R., Boivin, G. P., Cardell, E. L., and Doetschman, T. (1997) *Development* **124,** 2659–2670
15. Saika, S., Saika, S., Liu, C. Y., Azhar, M., Sanford, L. P., Doetschman, T., Gendron, R. L., Kao, C. W., and Kao, W. W. (2001) *Dev. Biol.* **240,** 419–432
16. Derynck, R., and Zhang, Y. E. (2003) *Nature* **425,** 577–584
17. Gromley, A., Churchman, M. L., Zindy, F., and Sherr, C. J. (2009) *Proc. Natl. Acad. Sci. U.S.A.* **106,** 6285–6290
18. Zindy, F., Williams, R. T., Baudino, T. A., Rehg, J. E., Skapek, S. X., Cleveland, J. L., Roussel, M. F., and Sherr, C. J. (2003) *Proc. Natl. Acad. Sci. U.S.A.* **100,** 15930–15935
19. Chytil, A., Magnuson, M. A., Wright, C. V., and Moses, H. L. (2002) *Genesis.* **32,** 73–75
20. Srinivasan, Y., Lovicu, F. J., and Overbeek, P. A. (1998) *J. Clin. Invest.* **101,** 625–634
21. Silva, R. L., Thornton, J. D., Martin, A. C., Rehg, J. E., Bertwistle, D., Zindy, F., and Skapek, S. X. (2005) *EMBO J.* **24,** 2803–2814
22. Zhao, S., and Overbeek, P. A. (2001) *Dev. Biol.* **237,** 45–53
23. Ittner, L. M., Wurdak, H., Schwerdtfeger, K., Kunz, T., Ille, F., Leveen, P., Hjalt, T. A., Suter, U., Karlsson, S., Hafezi, F., Born, W., and Sommer, L. (2005) *J. Biol.* **4,** 11
24. Itoh, S., Itoh, F., Goumans, M. J., and Ten Dijke, P. (2000) *Eur. J. Biochem.* **267,** 6954–6967
25. ten Hove, T., van den Blink, B., Pronk, I., Drillenburg, P., Peppelenbosch, M. P., and van Deventer, S. J. (2002) *Gut* **50,** 507–512
26. Seay, U., Sedding, D., Krick, S., Hecker, M., Seeger, W., and Eickelberg, O. (2005) *J. Pharmacol. Exp. Ther.* **315,** 1005–1012
27. Verdone, L., Agricola, E., Caserta, M., and Di Mauro, E. (2006) *Brief. Funct. Genomic. Proteomic.* **5,** 209–221
28. Clayton, A. L., Hazzalin, C. A., and Mahadevan, L. C. (2006) *Mol. Cell* **23,** 289–296
29. Sreeramaneni, R., Chaudhry, A., McMahon, M., Sherr, C. J., and Inoue, K. (2005) *Mol. Cell. Biol.* **25,** 220–232
30. Gomis, R. R., Alarcón, C., He, W., Wang, Q., Seoane, J., Lash, A., and Massagué, J. (2006) *Proc. Natl. Acad. Sci. U.S.A.* **103,** 12747–12752
31. Ewen, M. E., Sluss, H. K., Whitehouse, L. L., and Livingston, D. M. (1993) *Cell* **74,** 1009–1020
32. Cordenonsi, M., Dupont, S., Maretto, S., Insinga, A., Imbriano, C., and Piccolo, S. (2003) *Cell* **113,** 301–314
33. Hannon, G. J., and Beach, D. (1994) *Nature* **371,** 257–261
34. Aslanian, A., Iaquinta, P. J., Verona, R., and Lees, J. A. (2004) *Genes Dev.* **18,** 1413–1422

35. Inoue, K., Roussel, M. F., and Sherr, C. J. (1999) *Proc. Natl. Acad. Sci. U.S.A.* **96,** 3993–3998
36. Maeda, T., Hobbs, R. M., Merghoub, T., Guernah, I., Zelent, A., Cordon-Cardo, C., Teruya-Feldstein, J., and Pandolfi, P. P. (2005) *Nature* **433,** 278–285
37. Bouchard, C., Lee, S., Paulus-Hock, V., Loddenkemper, C., Eilers, M., and Schmitt, C. A. (2007) *Genes Dev.* **21,** 2775–2787
38. Seoane, J., Le, H. V., Shen, L., Anderson, S. A., and Massagué, J. (2004) *Cell* **117,** 211–223
39. Brunet, A., Bonni, A., Zigmond, M. J., Lin, M. Z., Juo, P., Hu, L. S., Anderson, M. J., Arden, K. C., Blenis, J., and Greenberg, M. E. (1999) *Cell* **96,** 857–868
40. Bulavin, D. V., Phillips, C., Nannenga, B., Timofeev, O., Donehower, L. A., Anderson, C. W., Appella, E., and Fornace, A. J., Jr. (2004) *Nat. Genet.* **36,** 343–350
41. Kimoto, K., Nakatsuka, K., Matsuo, N., and Yoshioka, H. (2004) *Invest Ophthalmol. Vis. Sci.* **45,** 2431–2437
42. Meyer-Ter-Vehn, T., Gebhardt, S., Sebald, W., Buttmann, M., Grehn, F., Schlunck, G., and Knaus, P. (2006) *Invest Ophthalmol. Vis. Sci.* **47,** 1500–1509
43. Thornton, J. D., Swanson, D. J., Mary, M. N., Pei, D., Martin, A. C., Pounds, S., Goldowitz, D., and Skapek, S. X. (2007) *Invest Ophthalmol. Vis. Sci.* **48,** 491–499
44. Wagner, E. F., and Nebreda, A. R. (2009) *Nat. Rev. Cancer* **9,** 537–549
45. Euler-Taimor, G., and Heger, J. (2006) *Cardiovasc. Res.* **69,** 15–25
46. Ross, S., Cheung, E., Petrakis, T. G., Howell, M., Kraus, W. L., and Hill, C. S. (2006) *EMBO J.* **25,** 4490–4502
47. Sebastian, T., Malik, R., Thomas, S., Sage, J., and Johnson, P. F. (2005) *EMBO J.* **24,** 3301–3312
48. Sebastian, T., and Johnson, P. F. (2009) *Cancer Res.* **69,** 2588–2598
49. Bhoumik, A., and Ronai, Z. (2008) *Cell Cycle* **7,** 2341–2345
50. Lin, A. E., Biglan, A. W., and Garver, K. L. (1990) *Ophthalmic Paediatr. Genet.* **11,** 121–122
51. Wang, M. K., and Phillips, C. I. (1973) *Acta Ophthalmol.* **51,** 434–437
52. Khaliq, S., Hameed, A., Ismail, M., Anwar, K., Leroy, B., Payne, A. M., Bhattacharya, S. S., and Mehdi, S. Q. (2001) *Invest Ophthalmol. Vis. Sci.* **42,** 2225–2228
53. de Larco, J. E., and Todaro, G. J. (1978) *Proc. Natl. Acad. Sci. U.S.A.* **75,** 4001–4005
54. Marquardt, H., Hunkapiller, M. W., Hood, L. E., Twardzik, D. R., De Larco, J. E., Stephenson, J. R., and Todaro, G. J. (1983) *Proc. Natl. Acad. Sci. U.S.A.* **80,** 4684–4688
55. Vijayachandra, K., Higgins, W., Lee, J., and Glick, A. (2009) *Mol. Carcinog.* **48,** 181–186
56. Young, N. P., and Jacks, T. (2010) *Proc. Natl. Acad. Sci. U.S.A.* **107,** 10184–10189
57. Alexandrow, M. G., and Moses, H. L. (1995) *Cancer Res.* **55,** 1452–1457
58. Derynck, R., Akhurst, R. J., and Balmain, A. (2001) *Nat. Genet.* **29,** 117–129
59. Ki, K. D., Tong, S. Y., Huh, C. Y., Lee, J. M., Lee, S. K., and Chi, S. G. (2009) *J. Gynecol. Oncol.* **20,** 117–121
60. Katuri, V., Tang, Y., Marshall, B., Rashid, A., Jogunoori, W., Volpe, E. A., Sidawy, A. N., Evans, S., Blay, J., Gallicano, G. I., Premkumar, Reddy, E., Mishra, L., and Mishra, B. (2005) *Oncogene* **24,** 8012–8024
61. Kiss, A., Wang, N. J., Xie, J. P., and Thorgeirsson, S. S. (1997) *Clin. Cancer Res.* **3,** 1059–1066
62. Murata, M., Matsuzaki, K., Yoshida, K., Sekimoto, G., Tahashi, Y., Mori, S., Uemura, Y., Sakaida, N., Fujisawa, J., Seki, T., Kobayashi, K., Yokote, K., Koike, K., and Okazaki, K. (2009) *Hepatology* **49,** 1203–1217